Aust. J. Phys., 1995, **48**, 79–87

A Fibre Optic Sensor for High-velocity Measurements of Projectiles Driven by Hot Gases

Frank Di Marzio,[A,C] *Jakub Szajman*[A] *and Alex Mazzolini*[B]

[A] Optical Technology Research Laboratory, Department of Applied Physics,
Victoria University of Technology, PO Box 14428, MMC,
Melbourne, Vic 3000, Australia.
[B] Department of Physics, Swinburne University of Technology,
John St, Hawthorn, Vic 3122, Australia.
[C] Present address: School of Physics, University of Melbourne, Parkville,
Vic 3052, Australia.

Abstract

A fibre optic sensor system for the measurement of the velocity of projectiles propelled by hot gases has been developed. It was found that fibre optic techniques have significant advantages over conventional breakwire methods in this electromagnetically noisy environment. A simple passive fibre system produced both accurate and reliable measurements of projectile velocities which, in this study, were in the range 1–3 km s^{-1}. In addition, by using a number of fibres at different positions along the projectile path, the average velocity of the projectile can be determined at several points, and a velocity profile for the projectile motion obtained.

1. Introduction

Optical fibres have been used in a multitude of sensing applications (Giallorenzi *et al.* 1982; Krohn 1988; Dakin and Culshaw 1988). The main advantages of fibre optic sensors are their immunity to electromagnetic interference (EMI), high accuracy, small size and economy. Indeed, optical fibre sensors have direct application in scientific instrumentation used for the measurement of temperature (Kyuma *et al.* 1982) and pressure (Bucaro and Cole 1979), as well as for Doppler velocimetry (Menon 1986) and magnetic field detection (Habner 1985).

An interesting application of fibre sensor technology is the measurement of the velocity of high-speed projectiles. A method of producing high-velocity polymer projectiles (flyer plates) is to vaporise a thin copper track by means of a rapid capacitive discharge of current (Logan *et al.* 1977; Richardson *et al.* 1988). The high pressure generated in the explosive vaporisation of the metal foil rapidly accelerates the thin polymer sheet through a collimating annulus. In this way, flyer plate velocities in excess of 1 km s^{-1} can be produced. The high-velocity flyer plates then impact on solid targets, generating shock waves, the characteristics of which are determined by both the properties of the target material and the velocity of the flyer plates.

The conventional method for determining these plate velocities involves 'time of flight' measurement using electrical breakwires strung across the path of the flyer (Podlesak 1993). A serious drawback with this method is the considerable uncertainty associated with breakwire timings in this electromagnetically noisy environment. To overcome or at least dramatically limit the effects of electromagnetic interference

0004-9506/95/010079$05.00

(EMI), a number of different optical fibre configurations were investigated. The details are given in the following sections.

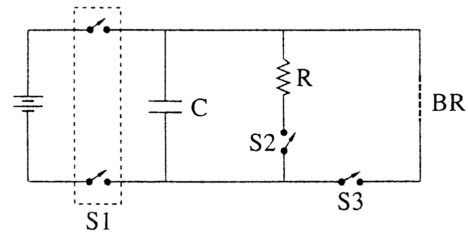

Fig. 1. Schematic diagram of the flyer plate generator. The capacitor and resistor are C and R respectively. S1 is the charging/isolation switch, S2 the current dump switch and S3 the firing switch for the bridge BR.

2. Equipment

The fibre optic velocity sensor has been designed for use on a large-scale 10 kV, 10 kJ flyer plate generator. However, in this study, a smaller 8 kV, 8 J generator was commissioned. The flyer plate generator utilises a $0 \cdot 25$ μF capacitor charged to a potential of 6 kV or 8 kV (Fig. 1), isolated, and then allowed to discharge a large current (in the order of 10 kA over a 1–2 μs interval) through a thin metallic conductor which rapidly heats and vaporises. The thin conductor is a 5 μm thick copper foil (bridge) which is bonded to a 35 μm thick polymer sheet. In the experiments reported in this paper, bridges with widths of $1 \cdot 5$ mm (small) and 3 mm (large) were used. When the bridge vaporises, the hot gases generated propel the polymer flyer towards the target. A tamper plate is located below the bridge to direct the hot gases driving the flyer upward through the annulus (Fig. 2).

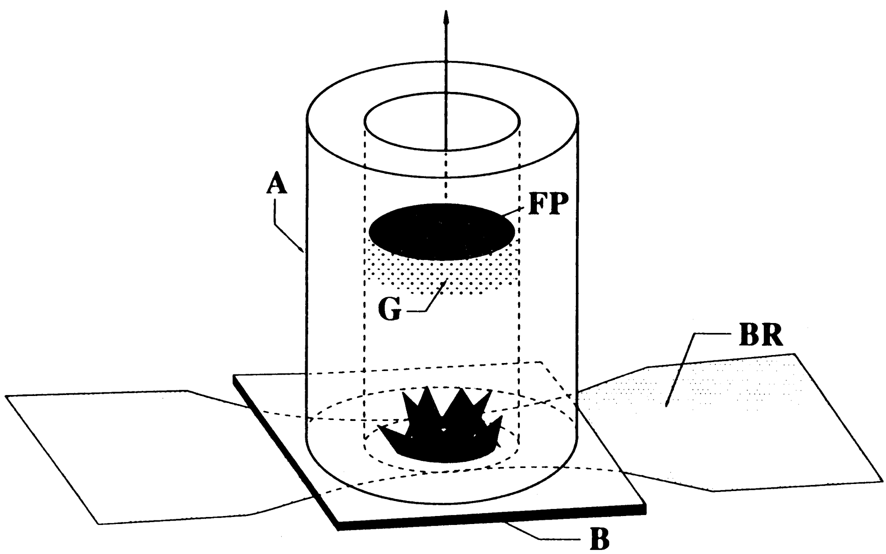

Fig. 2. Vaporisation of the bridge BR produces hot gases G which propel the flyer plate FP through the annulus A. The barrel B generates a cleanly cut flyer plate.

In the past, the velocity of these flyer plates on the large rig was determined by detecting the breakage times of current-carrying wires placed in the path of the flyer. However, there is considerable inaccuracy in the electrical breakwire technique, as the large currents employed in the vaporisation of the bridge produce a high level of EMI which adversely affects the breakwire signals (Podlesak 1993). A typical breakwire result is displayed in Fig. 3. The time of breakage of the wire is difficult to estimate since the electromagnetic noise is comparable to the actual signal, which in turn leads to uncertainty of interpretation and potentially inconsistent results.

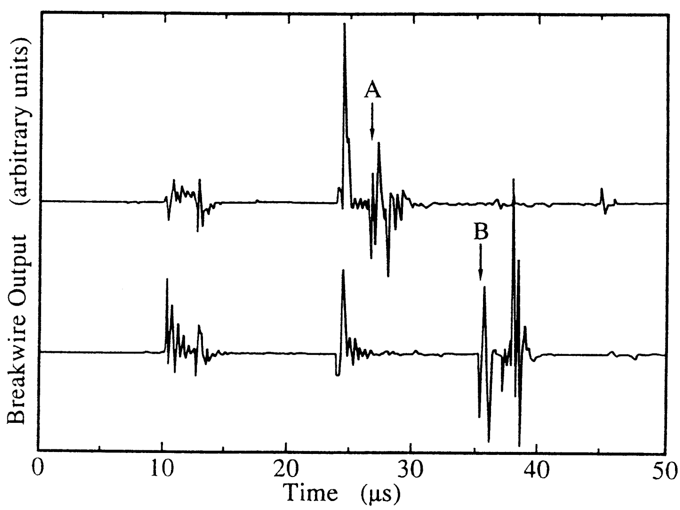

Fig. 3. A typical result showing the differential current through each wire in the electrical breakwire system. The instants of breakage of wires 1 and 2 are indicated by A and B respectively. The signals occurring at the same time correspond to noise.

In order to overcome these problems, a technique was developed which involved the replacement of current-carrying breakwires with EMI-immune optical fibres. Both a fibre breakwire system and a passive fibre sensor were investigated.

3. Fibre Optic Sensor System

(3a) Active Fibre Breakwire System

The velocity detection system can be significantly improved by replacing the current-carrying breakwires with optical fibres (Szajman *et al.* 1989). The initial experiments employed a HeNe laser as a light source and a reverse-biased fast photodiode detector, both of which were coupled to a multimode optical fibre breakwire. The detector output was recorded on a storage oscilloscope for analysis.

It was initially expected that as the polymer flyer shattered the fibre, laser light transmission would cease. In practice, the intense light generated by the hot gases directly beneath the fast-moving flyer coupled into the shattered fibre with a level far in excess to that provided by the 0·5 mW HeNe laser. Consequently, the laser light was found to be redundant since its signal was swamped by the light from the hot gases (Szajman *et al.* 1989). In all subsequent experiments, use of the laser was discontinued.

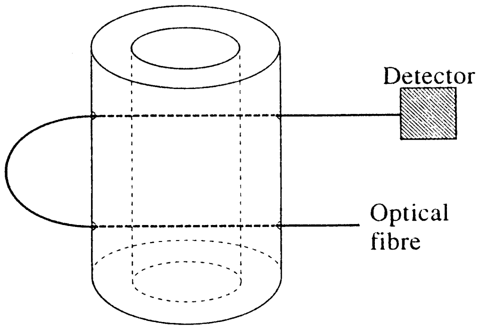

Fig. 4. The (invasive) fibre optic 'breakwire' system in the hairpin arrangement. The light emitted by the hot gases beneath the flyer plate provides the required signal.

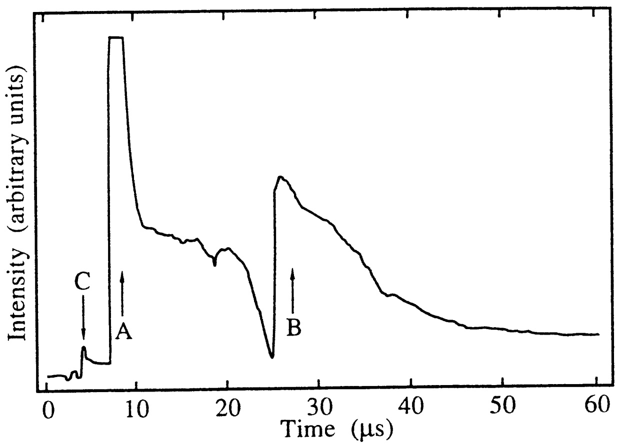

Fig. 5. Results obtained using the hairpin configuration show peaks due to light entering the shattered lower (A) and upper (B) fibre. The light generated from the initial bridge burst is also recorded (C).

The required time-of-flight signals can be obtained by using two separate fibre breakwires or a single fibre arranged in a hairpin configuration as shown in Fig. 4. A typical result for the latter system is displayed in Fig. 5. The large saturated peak (A) is due to light from the hot gases (beneath the flyer) entering the shattered lower section of the fibre. As the thin layer of gas propelling the flyer passes beyond the viewing angle of the fibre, the light intensity rapidly decreases until the upper section of the fibre is broken. At this time the light intensity increases again to form the second peak (B). It is worth noting that peak B is broader and less intense than peak A due to the expansion and cooling of the gas disk. The smallest peak (C) is due to the initial flash of light produced by the heating and consequent vaporisation of the bridge.

The average velocity of the flyer between the two optical breakwires was determined from the distance between the fibres and the time interval between the leading edges of the main peaks. One problem with this technique when used on the small rig is that the flyer loses considerable kinetic energy in breaking the optical fibres. On the larger (10 kJ) rig such energy losses are negligible, although on breakage, a section of fibre adheres to the flyer. The fibre may adversely affect the shockwave pattern generated as the flyer hits the target. Accordingly, a passive (non-invasive) fibre optic sensor was considered.

(3b) Passive Fibre Velocity Sensor and Its Resolution

A non-invasive method of velocity determination entails using the light emitted from the hot gases in order to obtain information without the need for breaking the optical fibre with the flyer. This passive fibre time-of-flight optical system is displayed in Fig. 6.

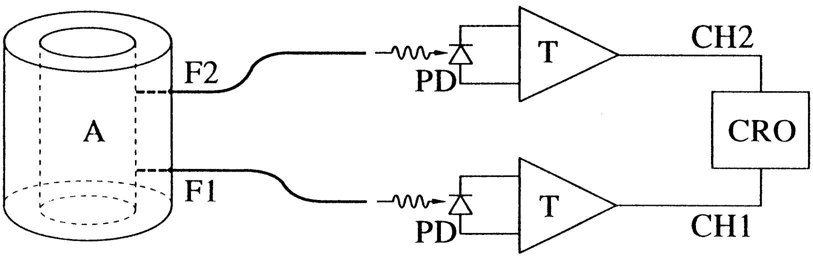

Fig. 6. Schematic for the passive optical fibre time-of-flight system. The signals acquired by the fibres (F1 and F2) are directed to the photodiodes (PD), amplified (T) and then stored in separate channels (CH1 and CH2) of the oscilloscope (CRO).

The 250 μm (50 μm core) fibres were stripped, cleaved and inserted into 0·3 mm diameter holes drilled into the side of the annulus. The fibre ends were aligned with the inner wall of the annulus and did not obstruct the motion of the flyer. The signals acquired in this manner were then detected by photodiodes and the events recorded on a storage oscilloscope.

The multimode fibre has a numerical aperture of 0·2 corresponding to a semiangle of 14°. Since the hollow section of the annulus has a diameter of 5·5 mm, the maximum vertical displacement viewed by the fibre is 2·2 mm. This viewing angle is reduced with the use of 8 μm core fibre (single-moded for light with wavelength greater than 800 nm), which translates to approximately twice the resolution.

The instrument resolution of such a passive fibre sensor is dramatically improved by the use of collimating cyclinders inserted up to the inner surface of the annulus. If the end of the fibre is slid inside the hollow cyclinder about 1 mm back from the inner edge, then the viewing angle for both single-mode and multimode fibre is predominantly governed by the collimating tube. In our experiments the fibre was withdrawn 2 mm from the tip of the collimator, thereby ensuring essentially identical resolution for both types of fibre.

A useful application of the velocity sensor is in the determination of the velocity distribution of the flyer as it travels upwards along the polycarbon annulus. This is discussed in the next section.

4. Results and Discussion

Our initial results were produced using the active fibre system. The laser level was totally submerged by the much greater signal entering the fibre after breakage, with the main signal being clipped due to saturation of the photodiode. It is interesting to note that light generated during the bridge burst can enter the fibre and produce a small prepeak. This prepeak can be used to establish the time at which the bridge vaporises and thus the average flyer velocity between the barrel and the first sensor.

Unfortunately, the small-scale flyer generator is severely limited by the energy loss incurred by the flyer in breaking the fibres. An example of this type of effect was demonstrated using a single fibre in a hairpin arrangement as shown in Fig. 4. Although this has the advantage of requiring only one input channel on the storage oscilloscope, energy losses experienced by the flyer are significant, as is evident in Fig. 5. The average velocity of the flyer between bridge burst and the first fibre (at a distance of 3·1 mm) was 720 m s^{-1} but between the two fibres (2·6 mm apart) this was reduced to 140 m s^{-1}. Accordingly, this type of velocity measurement technique is not suited to such a small rig. However, on the bigger rig the kinetic energy of the flyer is large enough to ensure that the energy losses due to fibre breakage are insignificant.

The passive fibre system does not suffer from these drawbacks and was employed in most of our analyses. It is important to note that the width of the peaks of the subsequent results is not necessarily an indication of instrument resolution, but a consequence of the shape and brightness of the hot gas propelling the flyer.

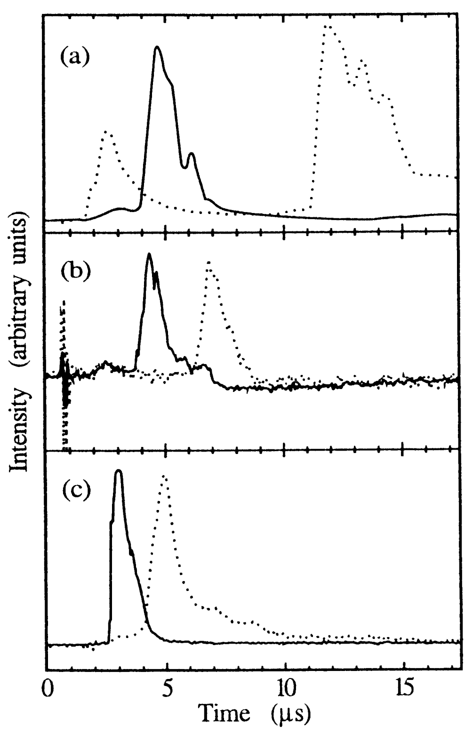

Fig. 7. (*a*) A typical result obtained using the passive optical fibre system. The average flyer velocity between the first and second sensor was determined to be 1140 m s^{-1}. A large bridge and multimode fibre was used in this experiment. (*b*) Single-mode fibre result obtained using a large bridge. In this case the average velocity between the fibres was 1250 m s^{-1}. (*c*) Single-mode fibre result obtained using a small bridge. This smaller bridge generated a faster flyer with an average velocity of 2120 m s^{-1}.

An example of the spectrum obtained using two passive sensors is presented in Fig. 7*a*. The average velocity (over 4·0 mm) between the prepeak and the main peak was 1540 m s^{-1}, whereas between the two fibres (8·0 mm apart) it was found to be 1140 m s^{-1}. These results were taken using 50 μm core optical fibre and a large bridge. Again, a prepeak is observed as a consequence of the initial burst of light entering the fibre. Note that the variations of the flyer velocities (barrel to first sensor) in Fig. 7 and Fig. 5 are due to differences in the placement of the fibre sensors along the annulus.

The resolution of the optic fibre probe was significantly improved through the use of single-mode (8 μm core) fibre which has a viewing angle of approximately 6° (at a wavelength of 1300 nm). Although the reduction in core size from 50 μm to 8 μm decreases the intensity at the detector, even the 8 J rig maintains an excellent signal-to-noise ratio. This is borne out in the results of Fig. 7*b* in which the average velocity between the 8 μm core fibres (3·0 mm apart) was determined to be 1250 m s^{-1} (again with a large bridge). Small bridges usually resulted in higher-velocity flyers, as demonstrated in Fig. 7*c* in which the fibres are separated by 3·2 mm. The average velocity of the flyer between these two fibres was measured to be 2120 m s^{-1}.

Under identical experimental conditions, the rise times for 8 μm core fibres are less than the corresponding rise times for the 50 μm fibres. The use of collimating cylinders consistently improved the rise time even further, with values generally falling below 100 ns. Accordingly, the timing resolution is greatly improved and provides a more detailed picture of the intensity distribution of the layer of hot gas propelling the flyer. In all cases, the sensor closest to the bridge produces the sharper peak, suggesting that the disk of hot gas driving the flyer is expanding with time.

The passive velocity measurement technique can easily be extended to accommodate more fibre sensors, allowing the determination of a multipoint velocity profile over the flyer path. In this study, four fibres in collimating

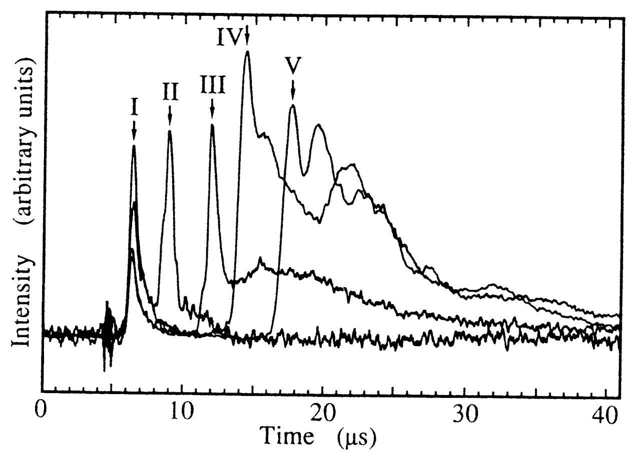

Fig. 8. The average velocity profile obtained using the passive fibre technique incorporating collimating cylinders and four fibres arranged vertically along the annulus. As the flyer passed each fibre, a signal was clearly recorded (II, III, IV and V). The common feature occurring at the same time (I) is the prepeak.

cylinders were placed vertically along the annulus. A number of velocity profile measurements were made using large bridges, while keeping the fibres in the same positions (at 1·58, 4·68, 7·40 and 10·60 mm ±0·04 mm from the barrel respectively). The results of one such measurement are displayed in Fig. 8. In all cases, the fibres were withdrawn 2 mm from the tips of the collimators.

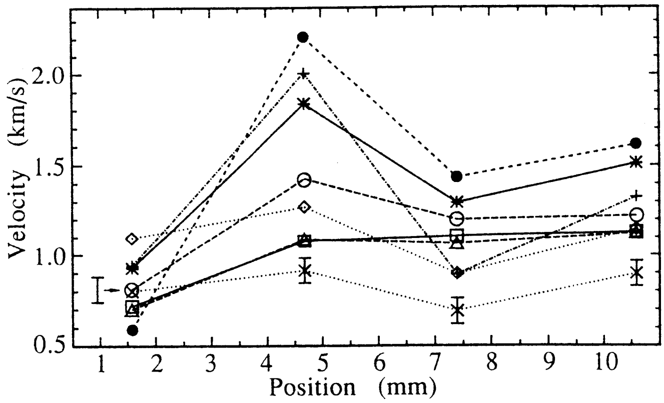

Fig. 9. Several velocity profiles derived from experiments using collimated optical fibres. In order to avoid congestion, error bars are included in only one set of data, but these are also representative of the error associated with the remaining profiles.

In each trace the prepeak can be clearly identified and allows an estimation of the minimum velocity between the barrel and the lowest fibre. The time at which the flyer passes each fibre sensor can be determined by extrapolating the leading edges of the main peaks down to the baseline. The resulting velocity profiles are presented in Fig. 9. The average velocity at position 1·6 mm (fibre closest to bridge) encompasses the primary acceleration of the flyer from rest and, as such, is expected to be smaller that subsequent velocity values. The difficulty in determining the precise position of each fibre is the main source of error, but this error amounts to less than the width of the data points displayed in Fig. 9.

5. Conclusions

A fibre optic sensor was found to provide a practical and accurate technique for the measurement of the velocity of flyer plates driven by hot gases. The system is essentially immune to electromagnetic interference and provides a reliable, non-invasive sensor capable of accurate measurements of high velocities. Considerable improvement in instrument resolution can be achieved through the use of collimating cyclinders, allowing singe-mode and multimode fibres to be employed interchangeably. In addition, the use of four optical fibres in tandem also provides information on velocity profiles.

Further, the experimental results suggest that the flyer is propelled by a thin disk of hot gas with the resultant full widths at half maximum of the main peaks showing a gradual increase as the flyer moves further away from the barrel. This implies that the hot gases are continually pushing the flyer away from the barrel and form a slowly expanding disk beneath the flyer.

Acknowledgments

Helpful discussions with Dr M. Podlesak are appreciated. Constructive comments from the referees are gratefully acknowledged.

References

Bucaro, J. A., and Cole, J. H. (1979). Conf. on Electronics and Aerospace Systems, Vol. 3, pp. 572–600 (IEEE: New York).

Dakin, J., and Culshaw, B. (1988). 'Optical Fibre Sensors: Principles and Components', Vols. I and II (Artech House: Boston).

Giallorenzi, T. G., Bucaro, J. A., Dandridge, A., Sigel, G. H., Cole, J. H., Rashleigh, S. C., and Priest, R. G. (1982). *IEEE J. Quantum Electron.* **QE–18**, 626.

Habner, R. E. (1985). Fibre optic applications in electrical power systems (Part 2). IEEE Tutorial Course (IEEE: Piscataway, N.J.).

Krohn, D. A. (1988). 'Fibre Optic Sensors—Fundamentals and Applications' (Instrument Society of America).

Kyuma, K., Tai, S., Sawada, T., and Nunoshita, M. (1982). *IEEE J. Quantum Electron.* **QE–18**, 676–9.

Logan, J. D., Lee, R. S., Weingart, R. C., and Yee, K. S. (1977). *J. Appl. Phys.* **48**, 621–8.

Menon, R. K. (1986). Proceedings of the ISA, Houston, TX, pp. 1185–95.

Podlesak, M. (1993). An exploding foil flying plate generator. Technical Report. (Defence Science and Technology Organization: Melbourne).

Richardson, D. D., Northeast, E. D., and Ryan, P. F. X. (1988). An exploding foil flying plate generator. Technical Report MRL-R-1133 DSTO Materials Research Laboratory, Australia.

Szajman, J., Di Marzio, F., Mazzolini, A., and Podlesak, M. (1989). Australian Conf. on Instrumentation and Measurement, Adelaide, p. 14 (IEA: Canberra).

Manuscript received 26 August, accepted 14 November 1994